NAGW-1631

NASA-CR-201444

A search for small solar-system bodies near the Earth using a ground-based telescope: technique and observations

L.A. Frank [1], J.B. Sigwarth [1], and C.M. Yeates [2]

[1] Department of Physics and Astronomy, The University of Iowa, Iowa City, IA 52242, USA
[2] Jet Propulsion Laboratory, California Institute of Technology, Pasadena, CA 91109, USA

Abstract. A large flux of heretofore undetected small comet-like bodies has been proposed by Frank et al. (1986a) in order to account for transient decreases of Earth's ultraviolet dayglow intensities. The inferred fluxes are sufficiently large to be detectable with moderately sized telescopes equipped with array detectors. Yeates (1989) has used the Spacewatch Camera at Kitt Peak National Observatory in a special operating mode in order to gain single images of small solar-system bodies near Earth. The detection is necessarily achieved near the threshold of the telescope. Further evidence for the existence of a large flux of small bodies in prograde, low-inclination orbits near Earth is reported here with the standard procedure of acquiring two consecutive images of the same small body with the Spacewatch Camera. A null test is performed in order to further demonstrate that the signatures in the images are not due to instrumental artifacts. Both our present results and those of Yeates (1989) provide tentative evidence that a large flux of small solar-system bodies is present at Earth's orbit and that the magnitude of this flux is similar to values inferred by Frank et al. (1986a). The number density is $3(\pm 1) \times 10^{-11}$ small bodies km^{-3}. The radii of these objects would be in the range of meters. An alternative interpretation is that these objects belong to a heretofore undetected population of naturally occurring satellites near geostationary orbits. The use of a telescope with larger aperture and/or array detectors with lesser noise levels is necessary to confirm the present observations.

Key words: small comets – observational methods – photometry

1. Introduction

Frank et al. (1986a, b) interpret transient decreases of Earth's ultraviolet dayglow intensities as seen in images from the satellite Dynamics Explorer 1 in terms of obscuration of the dayglow by water clouds from the disruption and subsequent rapid vaporization of heretofore undetected small comets at positions just above the atmosphere. An overview of this phenomenon and appropriate references are given by Frank and Craven (1988). The mass and radii of the small comets are inferred to be $\sim 10^{8}$ gm and ~ 6 m, respectively, and their orbital motion to be prograde and

near the ecliptic with a speed relative to Earth and outside of its gravitational field of ~ 10 km s^{-1} (Frank et al., 1986a, c). A possible source of these small comets is identified by Frank et al. (1986d) as an inner Oort disk of comets generally lying outside the planetary system and parallel to the ecliptic plane (Oort, 1950; Hills, 1981). Frank et al. (1987) have suggested that the mantle material, perhaps carbon-based, may be similar to that observed for the very dark surfaces of comet P/Halley (cf. Keller et al., 1986). The most controversial aspect of the interpretation of the dayglow decreases, also known as 'atmospheric holes', is the flux of small comets required to account for the observed occurrence rate of the dayglow events. The corresponding impact rate into Earth's atmosphere is $\sim 10^{7}$ yr^{-1}. Soter (1987) has noted that the proposed flux of these objects is sufficiently large that detection with telescopes equipped with array detectors should be possible. A search was not performed by Soter. The only published search for small solar-system bodies near Earth is given by Yeates (1989).

Yeates (1989) devised an unusual mode of operation of the Spacewatch Camera at Kitt Peak National Observatory in order to search for the small comets. The method employs motion of the telescope field-of-view such that the small bodies would be tracked along their orbits. Hence the search relied upon the inferred motion of the objects. Even with the proposed large fluxes, the detection rate was expected to be small and the luminosity of the small bodies was necessarily observed near the sensitivity threshold of the telescope and its array detector. These objects were not precisely tracked by the telescope field-of-view and appeared as short trails, or streaks, in the images. An intensive analysis of 171 images by Yeates (1989) revealed the trails of 36 objects that satisfied the criteria of rigorous statistical testing and considerations of other possible sources such as cosmic rays, satellite debris, and detector noise. Each of the 36 objects was detected in a single frame. Our present work provides further evidence of the presence of a large, previously undetected flux of small bodies near Earth by employing the standard technique of detection of an individual object in two consecutive frames. The observations are further tested by operating the telescope in a mode for which no trails of these objects are expected in the images.
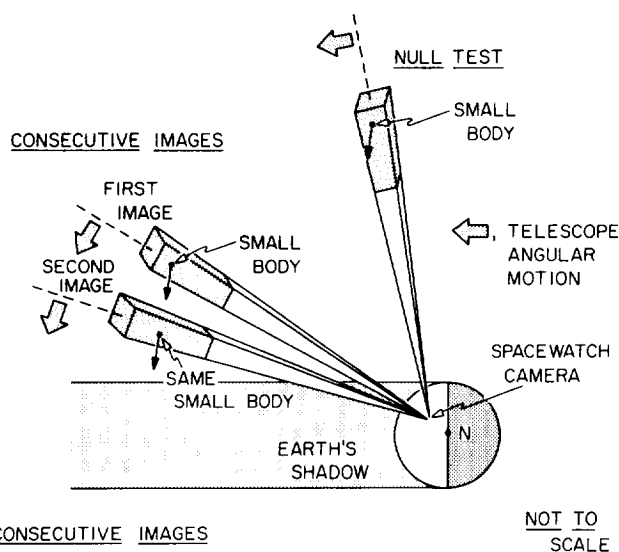
2. Method of observations

The Spacewatch Camera is a 36-inch Newtonian telescope located at Kitt Peak National Observatory at geographic coordinates 111° 36′0 W, 31° 57′8 N (Gehrels and Vilas, 1986; Gehrels et al.,

SPACEWATCH CAMERA

   - SEARCH FOR SMALL SOLAR-SYSTEM BODIES

NULL TEST

SMALL BODY

CONSECUTIVE IMAGES

FIRST IMAGE

SECOND IMAGE

SMALL BODY

TELESCOPE ANGULAR MOTION

SAME SMALL BODY

SPACEWATCH CAMERA

EARTH'S SHADOW

N

NOT TO SCALE

CONSECUTIVE IMAGES

IMAGE SAMPLE TIME: 12 SECONDS
NOMINAL TIME BETWEEN IMAGES: 36 SECONDS

REQUIREMENTS FOR DETECTION OF SMALL BODY

TRAILS MUST BE:

(1) COLLINEAR
(2) SAME LENGTH
(3) SAME BRIGHTNESS
(4) SEPARATED BY 3 TIMES THE TRAIL LENGTH

Fig. 1. Viewing geometries for the Spacewatch Camera for the acquisition of consecutive frames and for the null test on April 19, 1988

1986). An RCA SID 53612 charged-coupled array detector is used to provide images over a field-of-view of 0.25×0.16. The corresponding field-of-view of each of the 512×320 square pixels in the array is 1.77×1.77 (Gehrels et al., 1987). The method for pointing the telescope during the small body search is shown in Fig. 1 and has been discussed in detail by Yeates (1989). These objects are assumed to be streaming by Earth in prograde, low inclination motion with relative speeds of $\sim 10 \, \mathrm{km \, s^{-1}}$. The telescope field-of-view is moved with an angular rate that would approximately track the small body at a distance that corresponds to an apparent visual magnitude near the threshold of the telescope for detection of the small body. This maximum range is used because the volume for detection of the objects varies as $\varDelta^3$ where $\varDelta$ is the range from the telescope (Yeates, 1989). By coincidence the appropriate angular rate is approximately the sidereal rotation rate, $72.9 \, \mu \mathrm{rad \, s^{-1}}$, and the exposures are achieved by deactivating the telescope drive mechanism.

The duration of the exposure is determined by the read-out noise for the sensor, the dark current, and the sky background, e.g., the statistical fluctuations associated with increasing photo-site charge from dark current and sky background with longer exposures will eventually mask a dim trail from a small body. For the Spacewatch Camera the optimum exposure time for an image was found to be 12 s (Yeates, 1989). For example, a trail with length 10 pixels from a $18.^m6$ small body is near the threshold of the telescope. The average signal per pixel is approximately equal to 1 standard deviation σ for the background signal. For an apparent speed of $10 \, \mathrm{km \, s^{-1}}$ and a telescope angular motion of $72.9 \, \mu \mathrm{rad \, s^{-1}}$, the object would be tracked as a point at a range of

137000 km. If the same object leads or lags the field-of-view by $7.2 \, \mu \mathrm{rad \, s^{-1}}$ to form a 10-pixel trail in the image then the corresponding ranges are 125000 km and 152000 km, respectively. The cross section of the detection volume shown in Fig. 1 is $\sim 600 \times 380 \, \mathrm{km}$ at a range of 137000 km. Thus the detection volume corresponding to a single image is $\sim 6 \, 10^9 \, \mathrm{km^3}$, or only about 0.6% of Earth's volume. Thus it should be clear, even with this special technique, the volume density of objects must be large in order that any trails are to be detected.

The two consecutive images were each taken with a 12-s exposure time with a nominal interval of 36 s between images in order to accommodate read-out of the first image. The telescope drive is disabled during the entire sequence. Because this operation was manual, the pairs of images were checked as to exposure time and interval times by the lengths and positions of star trails in the pairs of images. Star trails are horizontal with constant length of 102 pixels for a 12-s exposure. After each pair of images was recorded the telescope was returned to the original pointing position in celestial coordinates in order to sample a new volume of space in the search for the small bodies. The requirements are highly constrained for detection of the same small body in consecutive images. The two trails must be the same length and visual magnitude, must be separated by three trail lengths, and must be collinear.

The observational periods and viewing coordinates for the search for small bodies near Earth are summarized in Table 1. The inclination to the ecliptic plane for the telescope motion is Earth-centered. For example, a small body that is captured in the field-of-view of the telescope during -19.4 motion with respect to the ecliptic on November 20 has an inclination to the ecliptic in inertial coordinates of -5.5. These inclinations ranged from -5.5 to 6.6 for the periods shown in Table 1. The first three periods shown in Table 1 are the observations used by Yeates (1989) to identify 36 trails in 171 images, each trail in a single image. Our present results were acquired on April 19, 1988. The null test is depicted in Fig. 1. The angular motion of the telescope field-of-view is directed perpendicular to the inferred motion of the small body. In this viewing geometry the trails would be approximately 100 pixels long and the responses per pixel would be too low to be detectable in an image. Also the apparent visual magnitude should be substantially reduced by the larger solar phase angle. No trails should occur in these frames if the trails are due to the inferred stream of small bodies. The two periods for acquisition of consecutive images of the small bodies are also shown in Table 1. Two viewing directions were used, one each for objects $160° \, E$ and $160° \, W$ of the Sun.

Because the image processing facilities for the Spacewatch Camera provide for a threshold detection level of $\sim 50 \, \mathrm{dn}$ (digitization units) per pixel (Gehrels and Vilas, 1986), special computer programs for processing and display of the images were implemented at The University of Iowa where the analyses were subsequently performed. The corresponding threshold level was reduced to $\sim 4 \, \mathrm{dn}$ per pixel. The event rate at the 4-dn threshold is about one each eight pairs of images. For the events recorded by Yeates (1989) the rate decreases by a factor of 10 per decrease of 1^m in apparent visual magnitude. Thus at the 50-dn threshold the event rate would have been about one event in 4000 image pairs, or one event about every 100 h of telescope operational time.

3. Observational results

With clear viewing conditions during the moonless night of April 19, 1988 a total of 69 pairs of images was attempted, 42 pairs

Table 1. Search periods for small bodies

Date	Universal Time	Right Ascension	Declination	Inclination to Ecliptic (Angular Motion)	Declination at Geostationary Orbit	Solar Phase Angle (Ecliptic Longitude)	Comments
20 Nov 1987	0233-0338	02h19m25s	13°55'00"	-19.4°	17°	20° (160°E)	Single images
20 Nov 1987	0814-0912	05h03m50s	22°41'00"	-5.5°	24°	20° (160°W)	Single images
23 Jan 1988	0556-0738	09h38m15s	14°06'43"	18.7°	17°	20° (160°W)	Single images
19 Apr 1988	0301-0451	08h45m00s	18°08'00"	15.5°	20°	80° (100°E)	Null test
19 Apr 1988	0703-0824	12h34m35s	-3°53'45"	23.1°	1°	20° (160°E)	Consecutive images
19 Apr 1988	0834-0924	15h08m00s	-17°45'00"	15.7°	-11°	20° (160°W)	Consecutive images
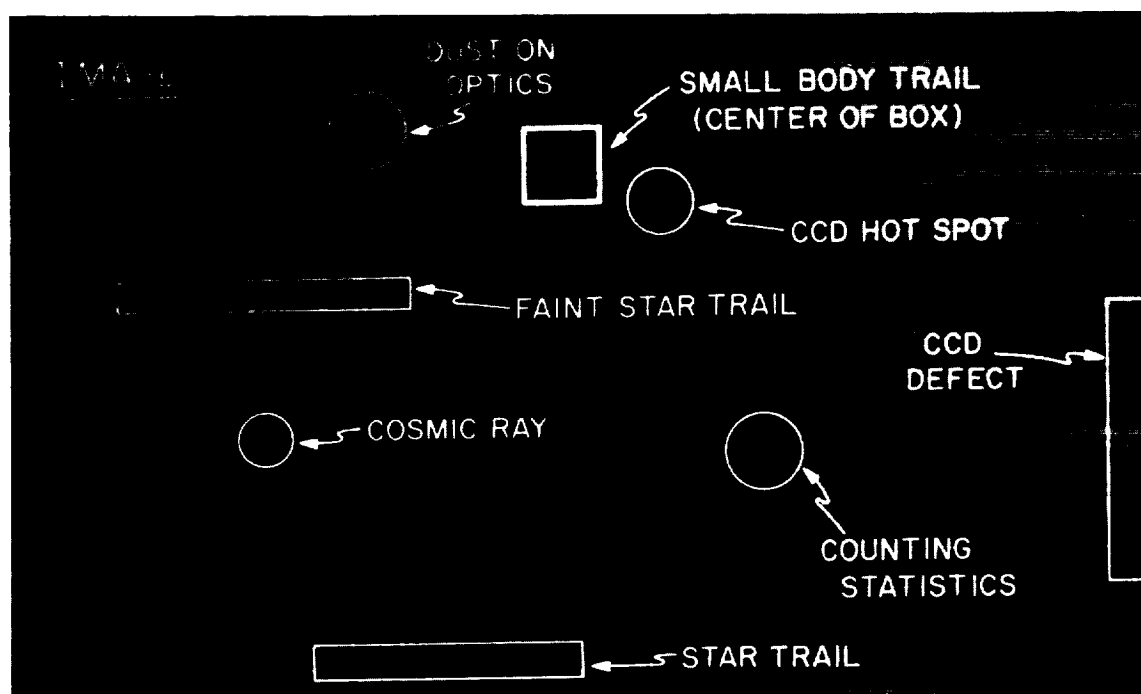
Fig. 2. Unprocessed image of a small-body trail (in center of box). Star trails and various instrumental artifacts are also identified. The exposure time is 12 s

at solar ecliptic longitude 160° E and 27 pairs at longitude 160° W (see Table 1). Due to loss of images from difficulties in manually controlling the telescope and exposure times, a total of 48 pairs of images was successfully acquired, 24 pairs each for the above two longitudes. An example of an unprocessed image with 12-s exposure time is given in Fig. 2. The gray code has been stretched in the range bracketing the photosite responses in order to search for the trails of small bodies. The laboratory displays are color coded and such trails are more easily identified. We present here a pair of unprocessed images in order to provide a visual impression

of the search task with the images. Standard techniques of spatial filtering can be used to enhance the trails but we reproduce the original images here for reference in future searches with other telescopes. Sensor defects, dust, ionization from a cosmic ray, and star trails are identified in Fig. 2. The apparent motion of the stars is to the left in the images. A faint star trail with pixel responses similar to those expected for the small body trails is also shown. This trail is necessarily uneven due to the counting statistics. A trail due to an unidentified small body is to be found in the center of the square in Fig. 2. The trail of this same object in the second
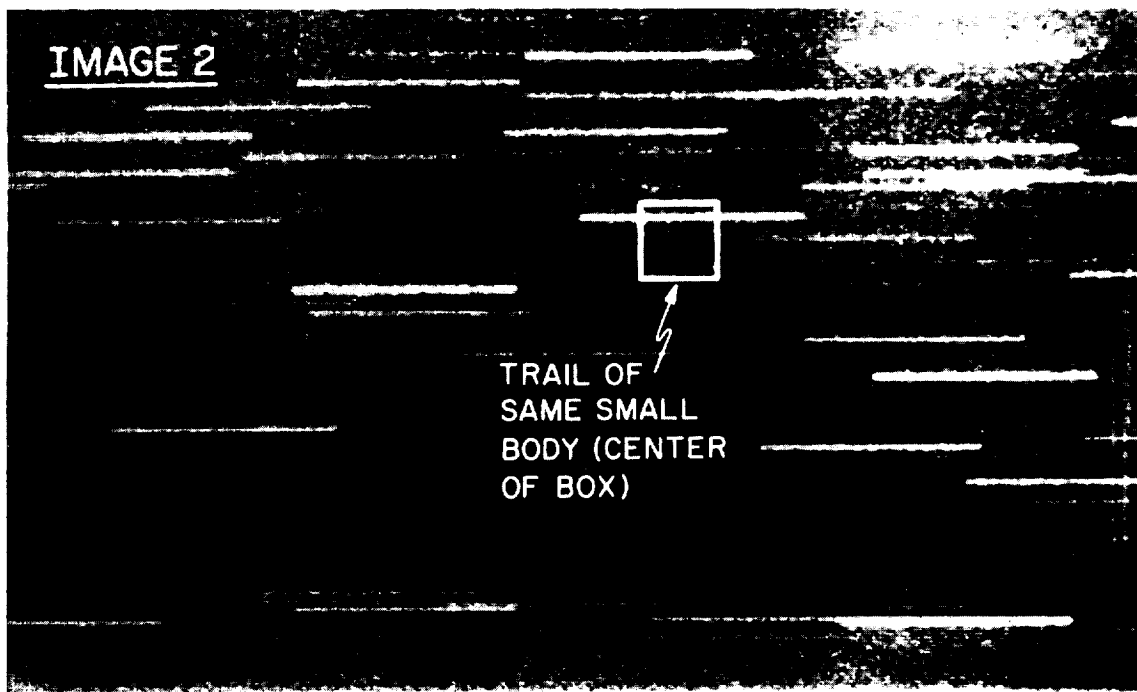
Fig. 3. A second unprocessed image of the trail of the small body identified in Fig. 2. This image was obtained during a 12-s exposure commencing 38 s after the exposure for the first image

image frame is shown in Fig. 3. This second image is exposed for a 12-s interval beginning 38 s after exposure of the first frame as the telescope field-of-view tracks the small body. Note that if either trail is positioned outside the field-of-view or crosses a star trail or sensor blemish then the pair is lost. These factors substantially reduce the field-of-view of the telescope for detection of the small bodies by a factor of 30% or more. Viewing directions with relatively few detectable stars were chosen in order to minimize these losses.

The pairs of images such as that shown in Figs. 2 and 3 are used to find the trails by visual inspection. Fulfillment of the stringent requirements for detection of the same object in consecutive images is verified with pixel maps of the residual responses for the trails. These pixel maps for Figs. 2 and 3 are shown in Fig. 4. A rectangular block of pixels that encompasses each trail is placed in the coordinates of the sensor array. These are residual responses after the subtraction of the average pixel response for a 1-pixel thick border. When this correction is not sufficiently accurate, then a "corrected" background response derived from all the pixels in the block, and excluding those in the trail, is used. The background varies slowly during the acquisition of a series of image pairs due to sensor temperature fluctuations. The subtracted background is about 140 dn with a standard deviation of ~ 4.6 dn for the entire image (see also Yeates, 1989). For the areas of the image that the trails are most easily detected the local standard deviation of pixel responses ranges from ~ 3.0 to 4.0 dn. The average increase of pixel responses above background shown for the two trails in Fig. 4 is 3.4 dn per pixel. The trail as defined here includes all pixels with centers within ±0.75 pixel of the visually determined best-fit line through the two trails. From calibration images with selected stars and the Palomar Observatory Sky Atlas (1954) it was determined that this width for the trails encompasses 75% of the total response. A total trail response of 75 dn corresponds to an apparent visual magnitude

$m_r = 18\overset{m}{.}6$. The accuracy for determination of the apparent visual magnitude of the small body is about $\pm 0\overset{m}{.}3$. Within statistical accuracy the visual magnitudes of the two trails shown in Fig. 4 are equal. The lengths of the two trails are also equal, 15 pixels each. The two trails are separated by 47 pixels which is the linear separation expected for the interval between exposures, which is 38 s for this example. The fourth fulfilled requirement for detection of the same small body is the collinearity of the trails.

An upper limit for the probability that the two trails shown in Fig. 4 are a random event can be set with the conservative assumption that all trails in the images are random events or artifacts. For example, there are only two 15-pixel trails in the 96 images. The number of possible orientations of a 15-pixel trail in the matrix of pixels is ~ 100. In order to randomly position these two trails such that they are at the expected separation and with collinear alignment in one consecutive image pair would require an ensemble of $8 \cdot 10^9$ image pairs. It is important to note that the technique of consecutive images of these dim objects directly eliminates the possibility of single independent events such as sensor noise, cosmic rays, and meteors as a source for the trails.

Pixel maps for five more detections of objects in consecutive frames are shown in Figs. 5 to 9 in the same format as Fig. 4. When a trail is observed in one image of the image pair it is detected in the other image unless the trail position is outside of the field-of-view or crosses a star trail or sensor blemish. The probability that these events are due to spurious effects is negligible. These probabilities are given in the figures and are determined in the same manner as that for Fig. 4. Motion of the small body to the left in these pixel maps corresponds to apparent angular motion that lags behind that of the telescope's field-of-view. Two small bodies were detected at 160° E of the sun, the remaining four bodies at 160° W (see the summary of events given in Table 2). The trails are oriented with a wide range of inclinations as viewed in the telescope reference frame. The trail lengths correspond to angular

RIGHT ASCENSION

DECLINATION

IMAGE I

DETECTION OF A 18.4^m SMALL BODY
IN CONSECUTIVE FRAMES WITH
THE SPACEWATCH CAMERA
RESIDUAL PIXEL MAPS
0837 UT, 19 APRIL 1988

TRAIL LENGTH: Ⓐ = Ⓑ

TRAIL BRIGHTNESS: Ⓐ Σdn = 82
(CORRECTED) Ⓑ Σdn = 92

PROBABILITY OF RANDOM OCCURRENCE
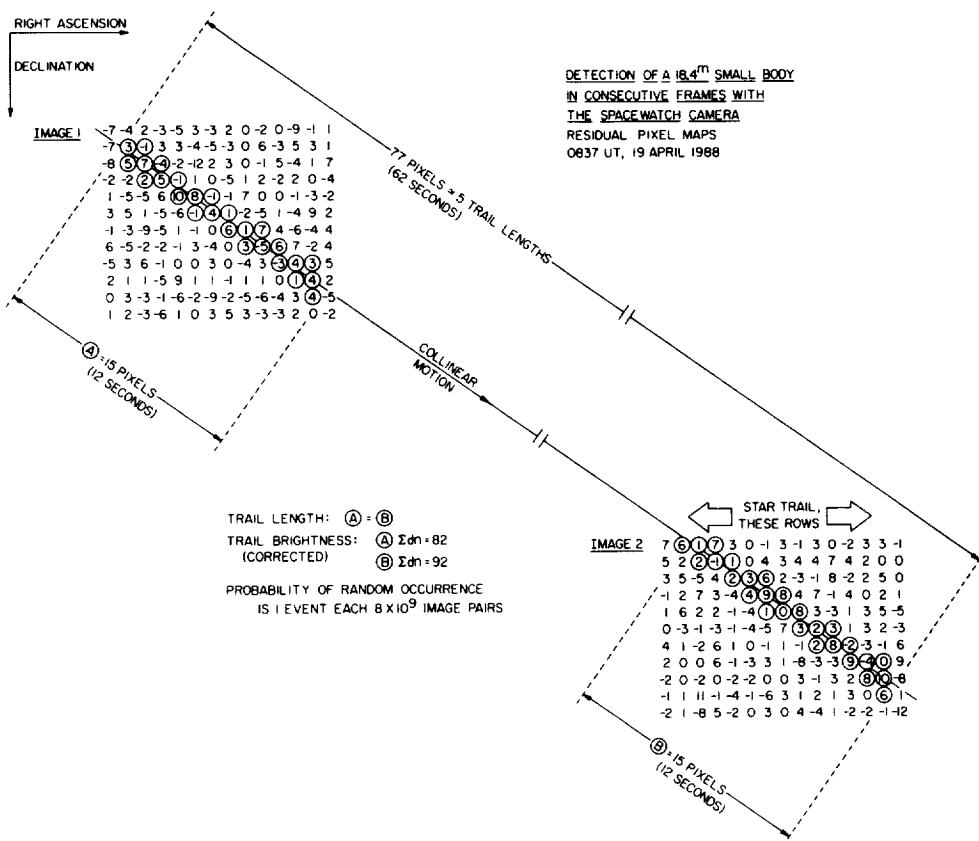IS I EVENT EACH 8 X 10^9 IMAGE PAIRS

IMAGE 2

Fig. 4. Pixel maps for the two trails of Figs. 2 and 3 in the coordinate system of the array detector. Residual responses above the average background are shown. The two trails satisfy the requirements for detection of the same object in consecutive frames: trails are (a) same length, (b) same brightness, (c) collinear, and (d) separated by 3 trail lengths
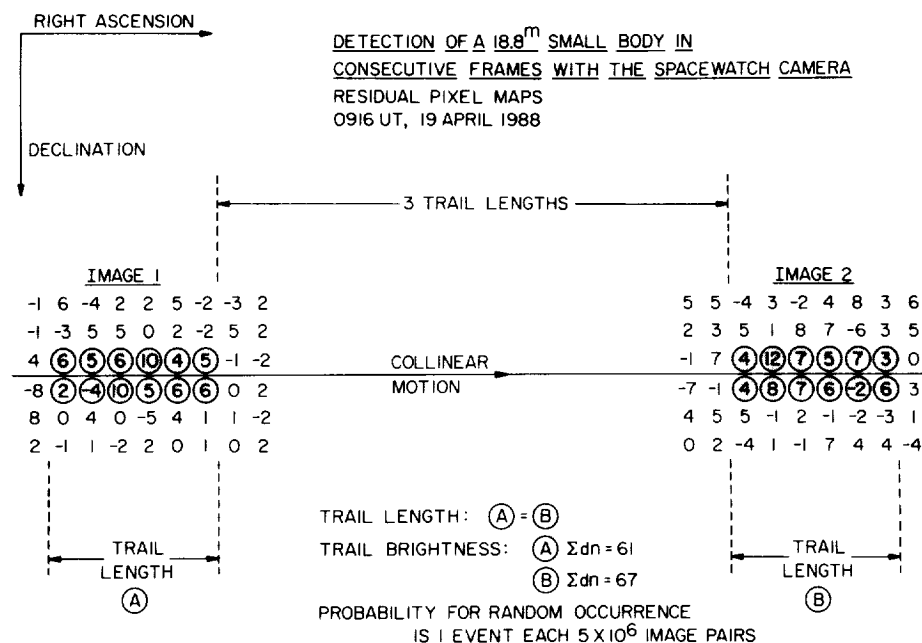
RIGHT ASCENSION

DETECTION OF A 18.8^m SMALL BODY IN
CONSECUTIVE FRAMES WITH THE SPACEWATCH CAMERA
RESIDUAL PIXEL MAPS
0916 UT, 19 APRIL 1988

DECLINATION

───── 3 TRAIL LENGTHS ─────

IMAGE I

```
-1  6 -4  2  2  5 -2 -3  2
-1 -3  5  5  0  2 -2  5  2
 4 ⑥⑤⑥⑩④⑤ -1 -2
-8 ②⊖④⑩⑤⑥⑥  0  2
 8  0  4  0 -5  4  1  1 -2
 2 -1  1 -2  2  0  1  0  2
```

COLLINEAR
MOTION

IMAGE 2

```
 5  5 -4  3 -2  4  8  3  6
 2  3  5  1  8  7 -6  3  5
-1  7 ④⑫⑦⑤⑦③  0
-7 -1 ④⑧⑦⑥⊖②⑥  3
 4  5  5 -1  2 -1 -2 -3  1
 0  2 -4  1 -1  7  4  4 -4
```

TRAIL LENGTH: Ⓐ = Ⓑ

TRAIL BRIGHTNESS: Ⓐ Σdn = 61
Ⓑ Σdn = 67

PROBABILITY FOR RANDOM OCCURRENCE
IS I EVENT EACH 5 X 10^6 IMAGE PAIRS

TRAIL LENGTH Ⓐ

TRAIL LENGTH Ⓑ

Fig. 5. Continuation of Fig. 4 for another small body

motions relative to the telescope of $0.7\,\mu$ rad s^{-1} per pixel of trail length.

The examination of the images taken during the null test shown in Fig. 1 was performed by an experienced viewer who was unaware that the images were taken at a solar phase angle of 80°. A total of 40 images was carefully examined and no trails were found. All of the images used in the present search were also inverted relative to the color scale, i.e., highest responses as black

and lowest responses as white, in order to search for pairs of identifiable "trails" for depressed rather than excess responses. No such trails were found.

4. Interpretation

Six small bodies with apparent visual magnitudes in the range of 19^m3 to 18^m4 were detected in 48 pairs of images (Table 2). The
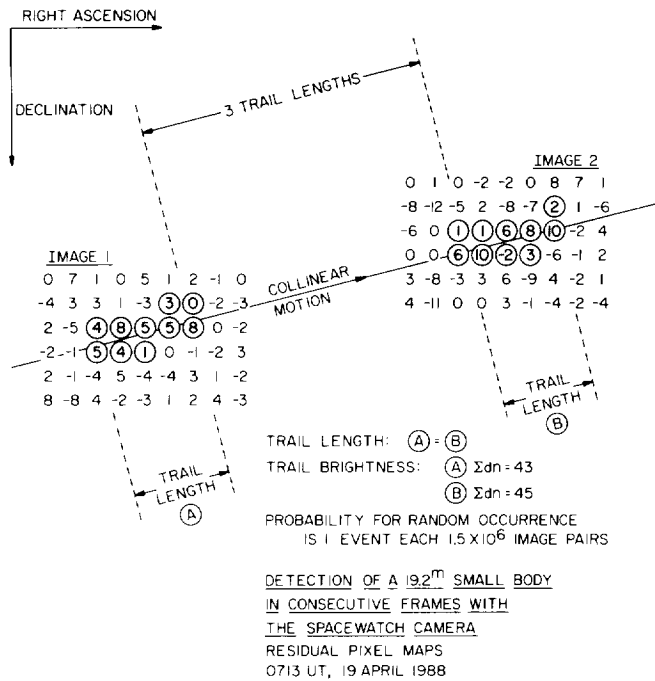
RIGHT ASCENSION

DECLINATION

3 TRAIL LENGTHS

IMAGE 2

```
0  1  0 -2 -2  0  8  7  1
-8 -12 -5  2 -8 -7  ②  1 -6
-6  0  ①①⑥⑧⑩ -2  4
0  0 ⑥⑩②③ -6 -1  2
3 -8 -3  3  6 -9  4 -2  1
4 -11  0  0  3 -1 -4 -2 -4
```

COLLINEAR MOTION

IMAGE 1

```
0  7  1  0  5  1  2 -1  0
-4  3  3  1 -3 ③⑩ -2 -3
2 -5 ④⑧⑤⑤⑧  0 -2
-2 -1 ⑤④① 0 -1 -2  3
2 -1 -4  5 -4 -4  3  1 -2
8 -8  4 -2 -3  1  2  4 -3
```

TRAIL LENGTH

Ⓐ

TRAIL LENGTH

Ⓑ

TRAIL LENGTH: Ⓐ = Ⓑ

TRAIL BRIGHTNESS: Ⓐ Σdn = 43
Ⓑ Σdn = 45

PROBABILITY FOR RANDOM OCCURRENCE
IS I EVENT EACH 1.5×10⁶ IMAGE PAIRS

DETECTION OF A 19.2ᵐ SMALL BODY
IN CONSECUTIVE FRAMES WITH
THE SPACEWATCH CAMERA
RESIDUAL PIXEL MAPS
0713 UT, 19 APRIL 1988

Fig. 6. Continuation of Fig. 4 for another small body

RIGHT ASCENSION

DECLINATION

3 TRAIL LENGTHS

IMAGE 1

```
-8  0 -2  2  6 -6  4  0
5 -8  5 -5 -1 -1 -6  2
2  2 -2  0  2  1 -3  1
-1 -1 -4  6 ④⑦ 1 -3
-4  2 ⑨⑦②③ -3 -4
-1  2 ⑩⑦ -1  0 -2 -6
4 -2 -2  2 -7 -6 -2  4
-1 -2 -2  0  0 -1  3 -1
```

COLLINEAR MOTION

IMAGE 2

```
-1  0 -3  4 -2 -1  0  4
6  0 -1  0 -3  0  2  1
5 -3  0 -3  2  4 10  1
-4  7 -2  5 ④⑥ 6  3
0  2 ⑥①⑩⑨  2  1
1 -1 ②⑩  2  2 -2  0
-5  2 -1  0 -7  3 -1  0
3 -3  1  3  0 -10  0  1
```

TRAIL LENGTH

Ⓐ

TRAIL LENGTH

Ⓑ

TRAIL LENGTH: Ⓐ = Ⓑ

TRAIL BRIGHTNESS: Ⓐ Σdn = 39
Ⓑ Σdn = 38

PROBABILITY FOR RANDOM OCCURRENCE
IS I EVENT EACH 7×10⁵ IMAGE PAIRS

DETECTION OF A 19.3ᵐ SMALL BODY
IN CONSECUTIVE FRAMES WITH
THE SPACEWATCH CAMERA
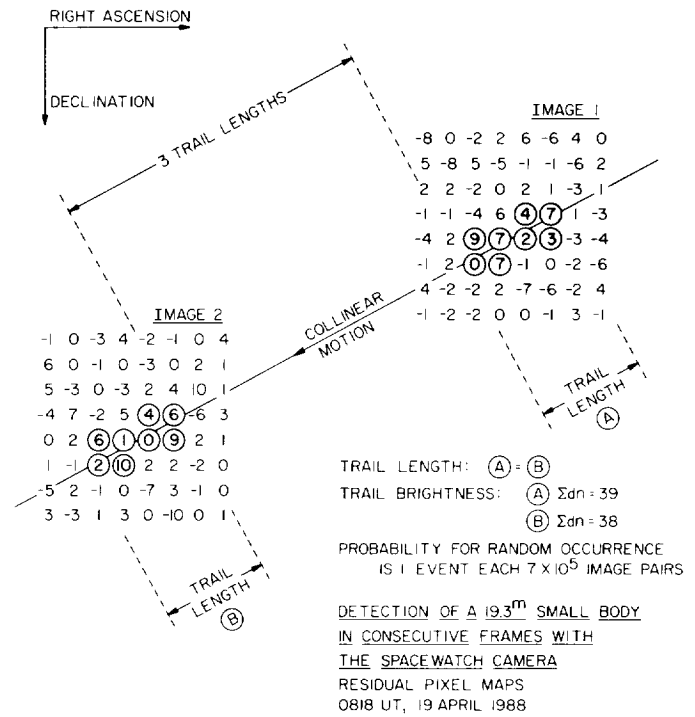RESIDUAL PIXEL MAPS
0818 UT, 19 APRIL 1988

Fig. 7. Continuation of Fig. 4 for another small body

Table 2. Detection of small bodies in 48 pairs of consecutive images

Universal Time, 19 April 1988	Solar Phase Angle	Apparent Angular Motion*, μrad/sec		Apparent Visual Magnitude	Probability of Random Occurrence, Upper Limit
		Right Ascension	Declination		
0713	160°E	+2.7(±0.2)	-0.8(±0.2)	19.2ᵐ	7×10^{-7}
0818	160°E	-2.5	+1.4	19.3ᵐ	1×10^{-6}
0837	160°W	+8.3	+6.9	18.4ᵐ	1×10^{-10}
0907	160°W	+4.4	-7.9	18.6ᵐ	2×10^{-9}
0908	160°W	-3.6	+0.4	18.9ᵐ	2×10^{-7}
0916	160°W	+4.2	0.0	18.8ᵐ	2×10^{-7}

*Relative to sidereal motion of telescope field-of-view.

trails of low-altitude man-made satellites and debris are too long to account for the short observed trails. Similarly the apparent angular motions of spacecraft and their debris in high-altitude orbits with moderate and high inclinations such as those of the Intelsat and Molniya series are too large to account for the short trails. We are then left with objects at distances ranging from the geostationary orbit and beyond. The apparent visual brightness m_v of an object at range Δ from the telescope is

$$m_v = m_s + 5\log\Delta - 2.5\log(r^2 p\Phi),$$

where $m_s = -26^m7$ for the Sun and r, p, and Φ are the radius, reflection parameter, and phase law, respectively, for the small body. For objects at geostationary orbit, $\Delta = 37000\,\text{km}$, the radius of the object as a function of apparent visual magnitude is shown in Fig. 10. The range of visual magnitudes reported by Yeates (1989) is also included in this figure. In order to find the limiting radii of the objects, the visual magnitudes for the brightest and darkest surfaces are given. The shaded area indicates our assessment of possible errors in determining these magnitudes: 0^m5 (solar color) $+0^m4$ (range) $+0^m6$ $(p\Phi) = 1^m5$. The solar

RIGHT ASCENSION
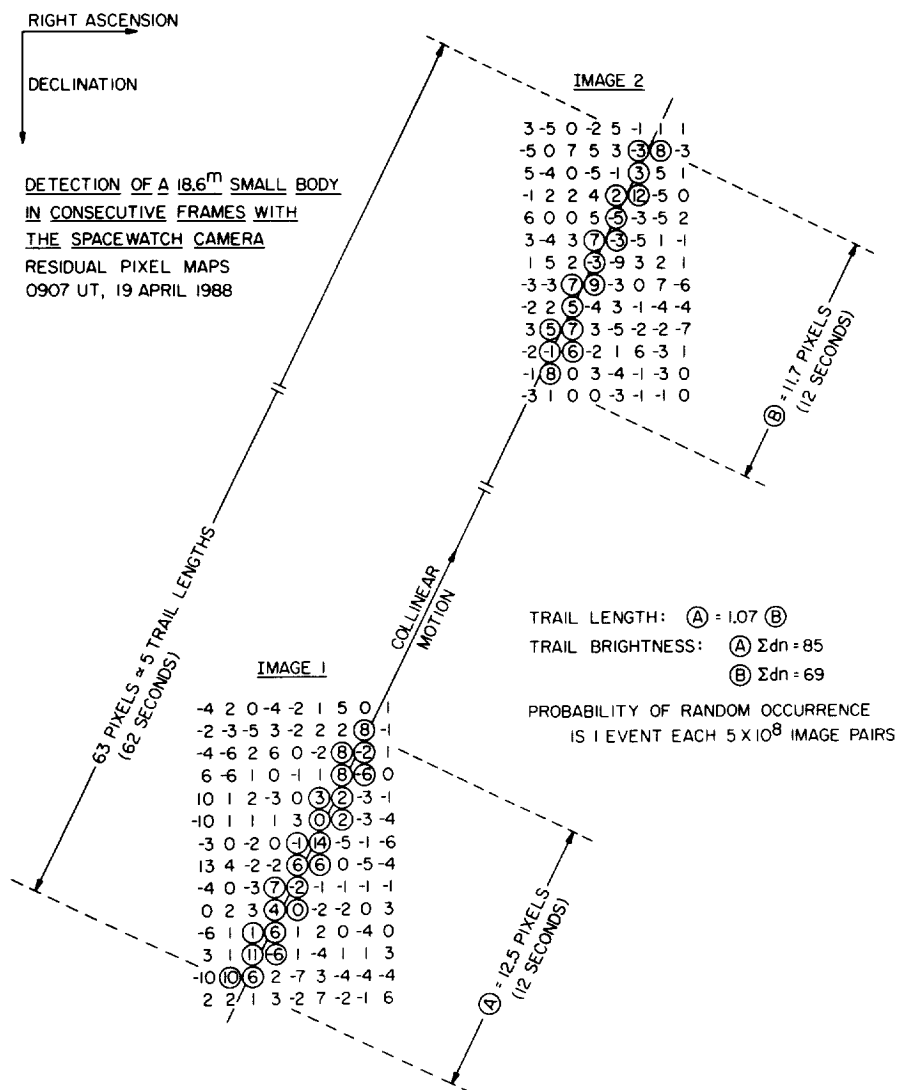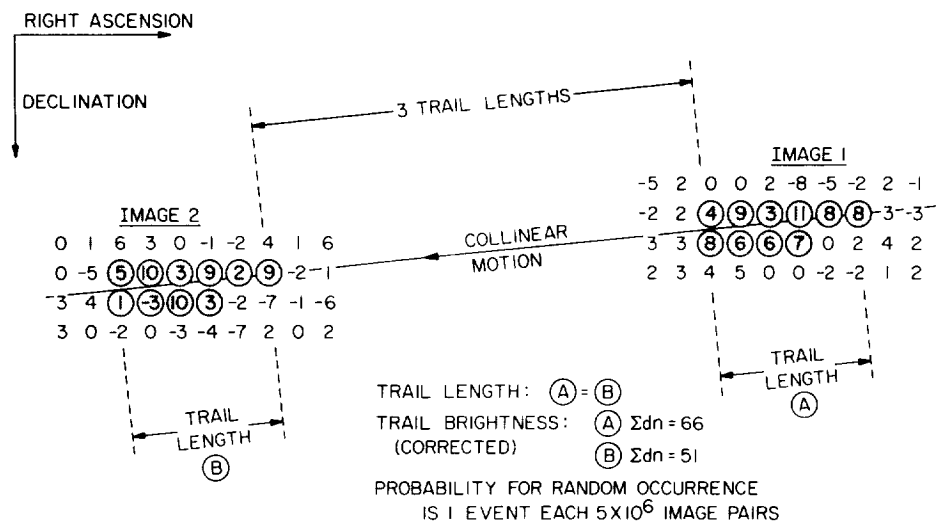
DECLINATION

DETECTION OF A 18.6ᵐ SMALL BODY
IN CONSECUTIVE FRAMES WITH
THE SPACEWATCH CAMERA
RESIDUAL PIXEL MAPS
0907 UT, 19 APRIL 1988

IMAGE 2

```
 3 -5  0 -2  5 -1  1   1
-5  0  7  5  3 ③⑧-3
 5 -4  0 -5 -1 ③ 5  1
-1  2  2  4 ②⑫-5  0
 6  0  0  5 ⑤-3 -5  2
 3 -4  3 ⑦③-5  1 -1
 1  5  2 ③-9  3  2  1
-3 -3 ⑦⑨-3  0  7 -6
-2  2 ⑤-4  3 -1 -4 -4
 3 ⑤⑦ 3 -5 -2 -2 -7
-2⑴⑥-2  1  6 -3  1
-1⑻ 0  3 -4 -1 -3  0
-3  1  0  0 -3 -1 -1  0
```

⑧ = 11.7 PIXELS
(12 SECONDS)

63 PIXELS = 5 TRAIL LENGTHS
(62 SECONDS)

COLLINEAR
MOTION

TRAIL LENGTH: Ⓐ = 1.07 Ⓑ

TRAIL BRIGHTNESS: Ⓐ Σdn = 85
                  Ⓑ Σdn = 69

PROBABILITY OF RANDOM OCCURRENCE
IS 1 EVENT EACH 5 X 10⁸ IMAGE PAIRS

IMAGE 1

```
-4  2  0 -4 -2  1  5  0/1
-2 -3 -5  3 -2  2  2 ⑧-1
-4 -6  2  6  0 -2⑻②1
 6 -6  1  0 -1  1⑻⑥0
10  1  2 -3  0③②-3 -1
-10  1  1  1  3 ⓪②-3 -4
-3  0 -2  0⑴⑭-5 -1 -6
13  4 -2 -2⑥⑥ 0 -5 -4
-4  0 -3⑦②-1 -1 -1 -1
 0  2  3④⓪-2 -2  0  3
-6  1 ⑴⑥ 1  2  0 -4  0
 3  1⑾⑥ 1 -4  1  1  3
-10⑽⑥ 2 -7  3 -4 -4 -4
 2  2/1  3 -2  7 -2 -1  6
```

Ⓐ = 12.5 PIXELS
(12 SECONDS)

Fig. 8. Continuation of Fig. 4 for another small body

RIGHT ASCENSION

DECLINATION

3 TRAIL LENGTHS

IMAGE 1

```
-5  2  0  0  2 -8 -5 -2  2 -1
-2  2 ④⑨③⑾⑧⑧-3 -3
 3 -3 ⑧⑥⑥⑦ 0  2  4  2
 2  3  4  5  0  0 -2 -2  1  2
```

COLLINEAR
MOTION

IMAGE 2

```
0  1  6  3  0 -1 -2  4  1  6
0 -5 ⑤⑽③⑨②⑨-2 -1
-3  4 ⑴-3⑽③-2 -7 -1 -6
3  0 -2  0 -3 -4 -7  2  0  2
```

TRAIL
LENGTH
Ⓐ

TRAIL
LENGTH
Ⓑ

TRAIL LENGTH: Ⓐ = Ⓑ

TRAIL BRIGHTNESS: Ⓐ Σdn = 66
(CORRECTED)   Ⓑ Σdn = 51

PROBABILITY FOR RANDOM OCCURRENCE
IS 1 EVENT EACH 5 X 10⁶ IMAGE PAIRS

DETECTION OF A 18.9ᵐ SMALL BODY IN CONSECUTIVE FRAMES
WITH THE SPACEWATCH CAMERA
RESIDUAL PIXEL MAPS
0908 UT, 19 APRIL 1988

Fig. 9. Continuation of Fig. 4 for another small body
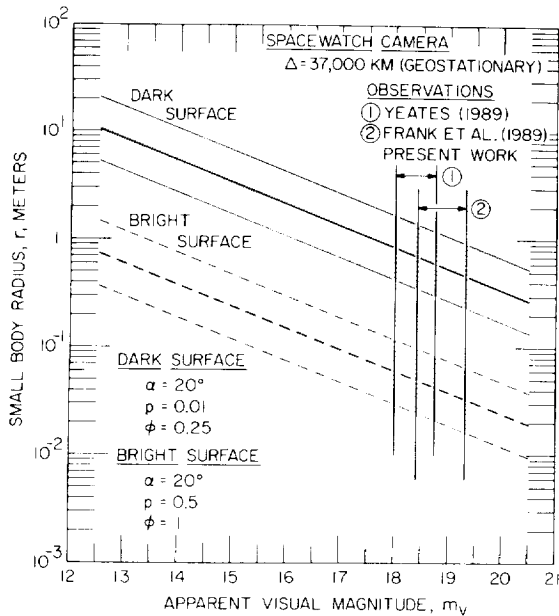
Fig. 10. Radius of a small body as a function of apparent visual magnitude m_v for two types of surfaces, bright and dark, as seen at a range $\Delta = 37\,000$ km corresponding to that of the geostationary orbit. The ranges of visual magnitudes for small bodies as reported in the present work and by Yeates (1989) are also identified

Fig. 11. Continuation of Fig. 10 for small bodies not bound in Earth's gravitational field at a range $\Delta = 137\,000$ km. The speed of these small bodies is assumed to be 10 km s^{-1} relative to Earth's orbital motion

phase angle $\alpha = 20$. For the dark surface we have assumed values of p appropriate for a dark carbon-based surface and a phase law Φ similar to that for Callisto (Allen, 1985). The range of radii corresponding to the observed visual magnitudes is ~ 2 cm to 2 m. However, the small, highly reflecting objects would have been probably detected during the null test at solar phase angle 80° if the phase law approximates the Lambert law ($q = 1.50$) or that for any higher value of phase law parameter q. A more reasonable lower limit on the radius is then probably 10 cm. The frequency of events reported here and by Yeates is ~ 5 trails deg^{-2}. The events are distributed over broad ranges of declination at geostationary orbit and right ascension (see Table 1). For a solid angle corresponding to $\pm 25 \times 360$, the observed occurrence rate of trails corresponds to a population of $\sim 10^5$ objects. The total population in the higher inclination orbits would be considerably greater because the telescope field-of-view does not track these objects along their entire orbits. For the purpose of obtaining a coarse estimate, if we assume that the mass density of these 10^5 objects is 3 g cm^{-3} and the object radius is 10 cm then the total mass of these objects would be $\sim 10^9$ g, or ~ 1000 tons. One of the viewing directions for consecutive images was directed nearly across the geostationary orbit (see Table 1). No increase in the frequency of detection of dim trails was found. We are unaware of any spaceflight program that has injected a large, uniform distribution of objects over such a wide range of declinations in nearly circular orbits at geostationary altitudes. From a survey with the Spacewatch Camera, Gehrels and Vilas (1986) have reported an upper limit for the number of objects with visual magnitudes 19^m to 13^m in geostationary orbit. This upper limit is ~ 0.1 object deg^{-2}, or a factor of ~ 50 less than the occurrence frequency for the observed trails. In summary there is no evidence that the trails reported here are due to man-made objects in the vicinity of the geostationary orbit.
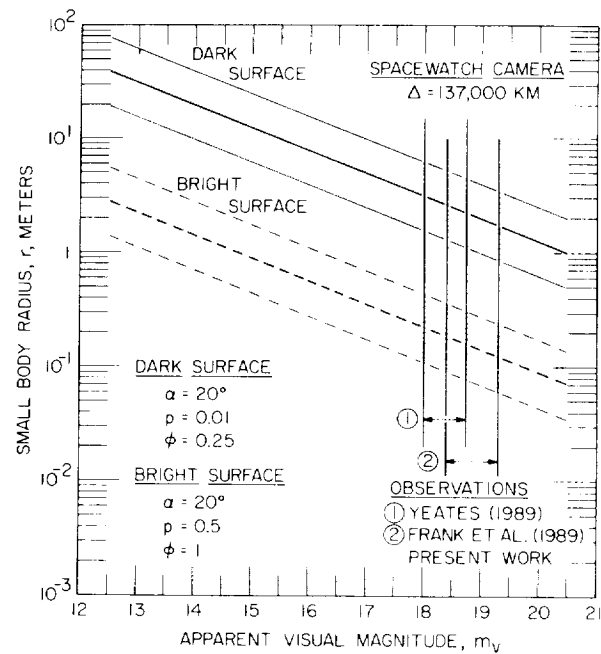
For objects significantly beyond geostationary altitudes the angular motion of the telescope corresponds to trajectories that are not bound in Earth's gravitational field. For objects bound in the solar gravitational well, and moving in prograde orbits near the ecliptic plane with perihelia in the vicinity of Earth's orbit, the maximum speed relative to Earth is ~ 12 km s^{-1}. If we assume that the typical speed is 10 km s^{-1} then the range Δ from the telescope to the objects is 137 000 km. The radii of objects that would account for the observed visual magnitudes at this range are shown in Fig. 11 in the same format as the previous Fig. 10. The size and flux of asteroid-type bodies can be estimated if they are assumed to be similar in mass density and optical properties to those of Ceres (Allen, 1985). The radius and mass of a Ceres-type object with visual magnitude 18^{m}8 are ~ 50 cm and $\sim 2 \times 10^6$ g, respectively. The number density of the observed objects can be determined from the detection volume per image pair (see Fig. 1) and the number of trails per frame. This number density is $3(\pm 1) \times 10^{-11}$ objects km^{-3}, or ~ 30 objects per Earth volume, and is similar to that reported by Yeates (1989). The corresponding impact rate for Earth is $\sim 10^7$ events yr^{-1}, with inclusion of the gravitational focusing factor. Dohnanyi (1978) reviews estimates of the impact rates of stony and iron meteors. For meteors with mass $\gtrsim 10^6$ g, the rates are ~ 2000 yr^{-1} (from fireball observations), ~ 50 yr^{-1} (estimate for stones), and ~ 0.5 yr^{-1} (lunar seismic data). Kyte and Wasson (1986) have recently attempted to consolidate several of these observations and obtained an estimate of ~ 10 objects yr^{-1} in the mass range 10^6 to 10^7 g. Although the above estimates vary over a large range, it is clear that stony and iron meteoroids cannot account for the large flux of small bodies that is reported here from the detection of their trails with the Spacewatch Camera.

The number density of small comet-like bodies has been inferred by Frank et al. (1986a, 1987) from the observed

occurrence rates of transient decreases in Earth's ultraviolet dayglow, or "atmospheric holes". The inferred densities ranged from $\sim 7 \ 10^{-11} \, km^{-3}$ in early November 1981 to a minimum of $\sim 7 \ 10^{-12} \, km^{-3}$ in mid-January 1982. These spatial densities are similar to the presently determined number densities of small bodies from trails in the images from the Spacewatch Camera, $3(\pm 1) \ 10^{-11}$ small bodies km^{-3}. Operation of the telescope was designed to track small solar-system bodies in low-inclination, prograde orbits with high eccentricity and perihelia near Earth's orbit as predicted from the observations of the motions of atmospheric holes (Frank et al., 1986c). The amount of water vapor necessary to obscure a sufficient area of ultraviolet dayglow to be detected with the imager on Dynamics Explorer 1 is $\sim 10^8 \, g$ (Frank et al., 1986a). For densities of water snow of 0.1 g and $0.3 \, g \, cm^{-3}$ the corresponding radii of the small comets before disruption and vaporization would be ~ 6 m and 4 m, respectively. If the small bodies detected with the Spacewatch Camera are the small comets proposed by Frank et al. (1986a), then the surface material must be dark (see Fig. 11).

An alternative interpretation of the small bodies may be a previously unidentified system of naturally occurring satellites in the vicinity of the geostationary orbit. The present observations cannot distinguish between the two classes of solar-system bodies.

5. Discussion

The Spacewatch Camera was operated in a special mode to obtain tentative identification of a heretofore unknown class of small solar-system bodies. These results provide evidence in support of similar findings reported by Yeates (1989) with single images of these objects. There are no previous telescope searches for small solar-system bodies near Earth. The presently determined number densities are $3(\pm 1) \ 10^{-11}$ small bodies km^{-3} if the objects are not gravitationally bound to Earth, or a population of greater than 10^5 naturally occurring satellites near geostationary orbit. The observed fluxes, orbital motions, and radii (if dark) of the small bodies detected with the telescope are in general agreement with those for the small comet-like objects previously inferred by Frank et al. (1986a–d, 1987) from the characteristics of transient decreases in Earth's ultraviolet dayglow. A total of 6 small bodies was unambiguously detected in a total of 48 pairs of images. The two consecutive images of each of the small bodies as reported here exclude the possibility that the observed trails are due to spurious single events such as cosmic rays, sensor noise, and meteors.

The lengths of the trails preclude their interpretation in terms of low-altitude spacecraft and their debris, or spacecraft and debris in eccentric, high-altitude orbits with moderate and high inclinations. The telescope field-of-view tracks geostationary objects or objects with greater speeds at larger distances. The density of the small body trails is a factor of at least 50 greater than that of objects with the same apparent visual magnitude in geostationary orbit. Thus, unless some spaceflight program pendent of the declination of the telescope field-of-view at the geostationary orbit. Thus, unless some spaceflight programm unknown to us has inserted a uniform distribution of more than 10^5 objects that are spread over a wide range of declinations of about $\pm 25°$ near the geostationary radius, then the trails are not due to man-made satellites and their orbital debris.

We have presented tentative evidence for the existence of a previously unknown class of small solar-system bodies near Earth.

The detection of these objects is performed at the sensitivity threshold of the Spacewatch Camera in order to acquire a useful event rate. The pairs of images were taken during a single night and the brightest small body was 18^m4. Several days of intensive analyses were required for this series of images. The detection of these objects at a modest increase of brightness 17^m0 with the Spacewatch Camera requires resources beyond those currently available to us. Because the event rate decreases by a factor of ~ 10 for each increase of 1^m, the acquisition of just 5 trails at 17^m0 or brighter would require about 125 times the number of images acquired for the present search. Thus the confirmation of the existence of these small solar-system bodies must await a similar search with another telescope with larger field-of-view, aperture, or a current-technology array detector.

References

Allen, C.W.: 1985, *Astrophysical Quantities*, The Athlone Press, London

Dohnanyi, J.S.: 1978, in *Cosmic Dust*, ed. J.A.M. McDonnell, Wiley, New York, p. 527

Frank, L.A., Craven, J.D.: 1988, *Rev. Geophys.* **26**, 249

Frank, L.A., Sigwarth, J.B., Craven, J.D.: 1986a, *Geophys. Res. Lett.* **13**, 307

Frank, L.A., Sigwarth, J.B., Craven, J.D.: 1986b, *Geophys. Res. Lett.* **13**, 303

Frank, L.A., Sigwarth, J.B., Craven, J.D.: 1986c, *Geophys. Res. Lett.* **13**, 1079

Frank, L.A., Sigwarth, J.B., Craven, J.D.: 1986d, *Geophys. Res. Lett.* **13**, 1484

Frank, L.A., Sigwarth, J.B., Craven, J.D.: 1987, *Geophys. Res. Lett.* **14**, 164

Gehrels, T., Vilas, F.: 1986, *Icarus* **68**, 412

Gehrels, T., Marsden, B.G., McMillan, R.S., Scotti, J.V.: 1986, *Astron. J.* **91**, 1242

Gehrels, T., Drummond, J.D., Levenson, N.A.: 1987, *Icarus* **70**, 257

Hills, J.G.: 1981, *Astron. J.* **86**, 1730

Keller, H.U., Arpigny, C., Barbieri, C., Bonnet, R.M., Cazes, S., Coradini, M., Cosmovici, C.B., Delamere, W.A., Huebner, W.F., Hughes, D.W., Jamar, C., Malaise, D., Reitsema, H.J., Schmidt, H.U., Schmidt, W.K.H., Seige, P., Whipple, F.L., Wilhelm, K.: 1986, *Nature* **321**, 320

Kyte, F.T., Wasson, J.T.: 1986, *Science* **232**, 1225

Oort, J.H.: 1950, *Bull. Astron. Inst. Neth.* **11**, 91

Palomar Observatory Sky Atlas: 1954, National Geographic Society, Washington, D.C.

Soter, S.: 1987, *Geophys. Res. Lett.* **14**, 162

Yeates, C.M.: 1989, *Planet. Space Sci.* (in press)